ISSN: 2790-5209 Vol 2, No.1, 2024

Study on the Properties of LiTaSiO5-based Lithium Ion Conductors Doped by Acceptors

Qi Ha [1], Qirui Zou [1], Xinyu Hu [1] and Weiguo Wang [1,*]

[1] College of Physics and Electronic Information, Yan'an University, Yan'an 716000, China.

* wwgissp@126.com

Abstract

Lithium-ion conductor plays an important role in the all-solid-state batteries. In this paper, the novel sphene structure LiTaSiO5 lithium-ion conductor material was taken as the research object. The lithium ion concentration can be changed by the acceptor doping of titanium ions. And further, the electrical properties of LiTaSiO5 lithium-ion conductor can be enhanced. Through the AC impedance spectroscopy measurement, the ion conductivity of Li1.1Ta0.9Ti0.1SiO5 sample can reach 1.93×10-5 S/cm at 333 K, which is higher than that of the parent LiTaSiO5 material at the same conditions. Combined with the results of dielectric relaxation spectroscopy, the higher ionic conductivity may be derived from the higher mobile lithium ion concentration in the Li1.1Ta0.9Ti0.1SiO5 compound. The research results have very important theoretical value for the research and design of new sphene-structure lithium-ion conductors.

Keywords

Lithium-ion conductor; Acceptor doping; Electrical conductivity; Mobile lithium ion con.

1. Introduction

Currently, commercial rechargeable lithium batteries use flammable liquid organic electrolytes, which pose risks of leakage, self-ignition, or detonation. Solid electrolytes themselves are leak free and non-flammable, so they can solve the safety issues of lithium batteries [1]. Despite decades of effort, only a small number of fast lithium-ion conductors have been discovered among numerous lithium-containing inorganic materials, including Li10GeP2S12-based compounds [2], argyroxene sulfides [3], garnet-like structures such as Li7La3Zr2O12 [4], Li1+xAlxTi2−x(PO4)3 [5], and perovskite types such as Li3xLa0.67−xTiO3 [6]. However, these lithium-ion conductors have limited stability in air or against lithium metals [7]. Therefore, it is still necessary to explore, discover and design new compounds with high ionic conductivity and excellent stability as solid electrolytes for all-solid-state lithium-ion batteries.

Recently, Hailong Chen et al. designed and synthesized a new lithium ion conductor with the structure of sphene using first principles calculation and in situ characterization techniques. The new conductor is based on the compound LiTaSiO5, which has a structure of sphenite, which has not previously been used for ionic conductor development and research [8]. By means of neutron diffraction, the characteristics of lithium ion occupancy in LiTaSiO5 compounds were determined, and the lithium ion conductivity of LiTaSiO5 materials was preliminatively studied, and it was found that undoped LiTaSiO5 materials showed very low ionic conductivity [8]. In order to improve the conductivity of ionic conductors, acceptor

doping is a common regulation method. In this paper, low-priced titanium ion (Ti4+) is used to replace high-priced tantalum ion (Ta5+), so as to achieve the purpose of regulating the concentration of lithium ion in LiTaSiO5 material. The structure, electrical properties and microscopic mechanism of lithium ion diffusion of Li1+xTa1-xTixSiO5 were studied by X-ray diffraction spectroscopy, AC impedance spectroscopy and dielectric relaxation spectroscopy.

2. Materials and methods

2.1. Sample preparation

High-purity lithium carbonate, titanium dioxide, tantalum pentoxide and silicon dioxide were used to prepare Li1+xTa1-xTixSiO5 (x=0 and x=0.1) samples by solid state reaction method. The specific preparation process is as follows: The experimental raw materials dried at high temperature were weighed according to the stoichiometric ratio, and an additional 10 wt.% lithium carbonate was added to make up for the loss in the process of high temperature synthesis and sintering. The weighed powder was put into the ball mill tank with anhydrous ethanol as the dispersant for 24h. The ball mill powder was dried in the air and pre-burned in the box Muffle furnace at 900℃ for 4h. The heating rate was 3℃/min. After the pre-fired powder continues to ball mill for 24h, calcined at 1000℃ for 24h, and cooled naturally with the furnace; The calcined powder was ball milled again for 24h, and the obtained powder was obtained by a uniaxial tablet press at about 350MPa pressure for the flake sample for electrical performance test. The obtained billets were put into the box type Muffle furnace for sintering at 1175℃ and the holding time was 24h. In order to reduce the volatilization of low melting point elements, the billet is covered with powder of the same composition.

2.2. Characterization methods

The powder X-ray diffractometer (XRD-7000, Shimadzu Corporation/JAPAN) was used to characterize the structure of the sintered samples. The Cu-Kα line was used as the X-ray diffraction source, and the test range was 20°-80°. The electrical properties of Li1+xTa1-xTixSiO5 (x=0 and x=0.1) Li-ion conductor samples were tested by an AC impedance analyzer (HIOKI IM 3536) with a frequency measurement range of 10 Hz-1 MHz and a temperature measurement range of 50-100℃. In order to ensure the stability of the measured impedance data, the sample Li1+xTa1-xTixSiO5 was held at each test temperature point for a period of time (about 20 min) before the impedance spectrum was tested.

3. Results and discussion

3.1. Structural analysis

As shown in Figure 1, Li1+xTa1-xTixSiO5 (x=0 and x=0.1) Li-ion conductor materials were tested at room temperature for X-ray diffraction spectroscopy (XRD). Compared with the standard PDF card (00-045-0644, LiTaSiO5), there is no new diffraction peak in either the parent phase LiTaSiO5 material or the 0.1mol Ti-doped Li1.1Ta0.9Ti0.1SiO5 sample. This indicates that titanium ions successfully entered the grid to form a solid solution having the structure of sphene.

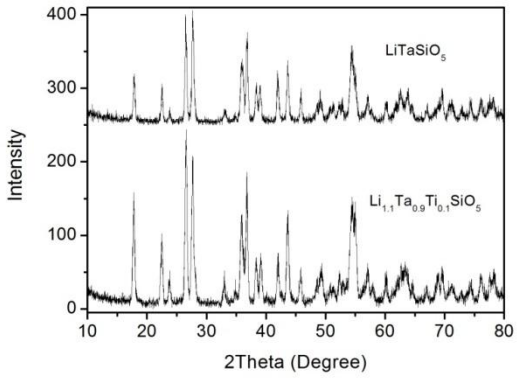

Figure 1: XRD patterns of the Li1+xTa1-xTixSiO5 (x=0 and x=0.1) samples

3.2. Ionic conductivity

Figure 2shows the AC impedance spectrum of Li1.1Ta0.9Ti0.1SiO5 lithium ion conductor sample at 60 ℃ . It can be seen from the figure that the impedance spectrum of Li1.1Ta0.9Ti0.1SiO5 sample is composed of three flattened semi-arcs, corresponding to the grain response, grain boundary response and electrode polarization response of the material from high frequency to low frequency in turn. An equivalent circuit composed of (R//CPE)(R//CPE//C)(CPE) was used to fit the AC impedance spectra of Li1.1Ta0.9Ti0.1SiO5 sample, where R is the resistor and CPE is the constant phase Angle element. Through equivalent circuit fitting, the order of grain capacitance and grain boundary capacitance reach 0.1 nF and 10 nF respectively, which is consistent with the order of grain capacitance and grain boundary capacitance of typical ionic conductors [9]. In addition, there is a 45-degree oblique upward linear ‘‘tail’’ in the low-frequency region of the impedance spectrum, which reveals the ionic conductive properties of Li1.1Ta0.9Ti0.1SiO5 sample. The grain resistance Rb of Li1+xTa1-xTixSiO5 lithium ion conductor sample can be obtained by nonlinear fitting method, and then the grain conductivity σb of the sample can be obtained according to the conductivity calculation formula σb=l/SRb.

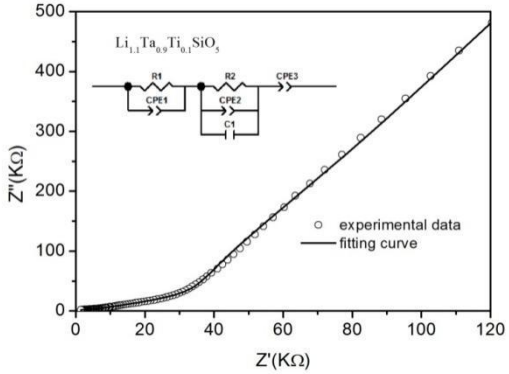

Figure 2: AC impedance spectrum and equivalent circuit fitting diagram of Li1.1Ta0.9Ti0.1SiO5 sample

Figure 3 shows the Arrhenius relation curve of grain conductivity of Li1+xTa1-xTixSiO5 (x=0 and x=0.1) with temperature. As can be seen from the figure, the grain conductivity of Li1+xTa1-xTixSiO5 (x=0 and x=0.1) materials showed a linear increase trend with the

increase of temperature. When the test temperature reaches 333 K, the grain conductivity of Li1.1Ta0.9Ti0.1SiO5 can reach 1.93×10-5 S/cm, which is nearly one data level higher than that of the parent LiTaSiO5 material at the same temperature (2.26×10-5 S/cm) [10].

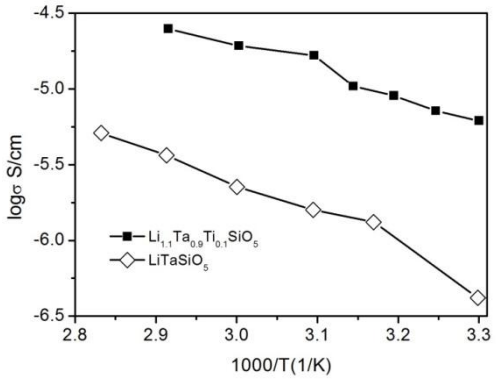

Figure 3: The Arrhenius curve of the bulk conductivity for the Li1+xTa1-xTixSiO5 (x=0 and x=0.1)

3.3. Dielectric relaxation spectrum

Figure 4 shows the relationship between dielectric loss of Li1.1Ta0.9Ti0.1SiO5 sample at different measurement temperatures (303 K, 308 K, 313 K and 318 K) and measurement frequency. A significant dielectric loss peak was observed in the measured frequency range. By changing the measured temperature, it is found that with the increase of the measured temperature, the peak position obviously moves to the high frequency region, showing typical characteristics of thermal relaxation peak [11]. From the fine characteristics of the dielectric relaxation peak, the peak is obviously composed of two small relaxation peaks (P1 peak and P2 peak). Two Debye peaks and an exponential background are used to fit the dielectric loss peaks by nonlinear fitting method. From the fitting effect, the total fitting curve has passed almost every experimental data point. Depending on the conditions under which the relaxation peak occurs ($\omega\tau=2\pi f\tau=1$), the relaxation time at different temperatures can be calculated. The Arrhenius relation ($\tau=\tau 0\exp（E/KT）$) curve of Li1.1Ta0.9Ti0.1SiO5 sample is shown in Figure. 5. It is obvious that the logarithm of relaxation time ($\ln\tau$) is linearly correlated with the reciprocal of the measured temperature (1/T). By linear fitting method, the relaxation activation energy parameters of the two relaxation peaks (P1 peak and P2 peak) are E1=0.31 eV and E2=0.35 eV, respectively.

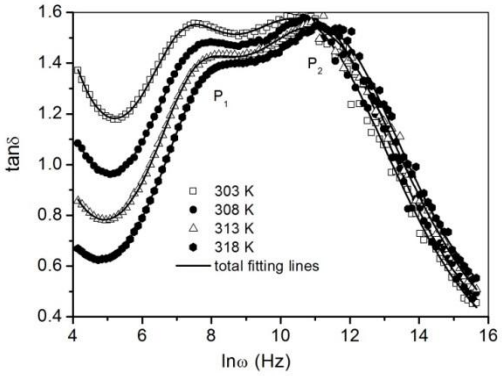

Figure 4: The curves and fitting lines of the dielectric loss tanδ versus lnw for

Li1.1Ta0.9Ti0.1SiO5 sample

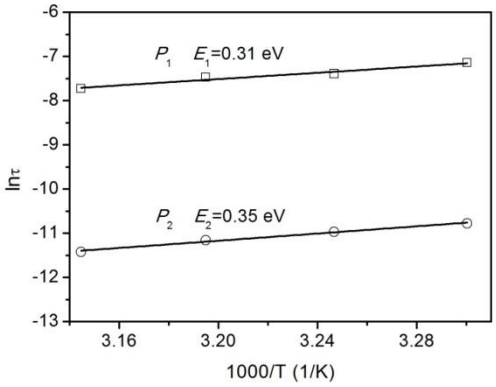

Figure 5: The Arrhenius curves of the Li1.1Ta0.9Ti0.1SiO5 sample in heating process

4. Discussion

The ionic conductivity of the Li1+xTa1-xTixSiO5 under the action of an electric field can be defined as the conductivity of diffusion and migration of lithium ions and lithium vacancy defects, which can be calculated using the Arrhenius equation [12]

$$\sigma = c_V \gamma l^2 \frac{q^2}{k_B T} \nu_0 \times e^{-\Delta E / k_B T} \qquad (1)$$

Among them, cV represents the lithium ion concentration, q refers to the charge of the carrier, l is the jump distance, γ is the geometric factor of lithium ion jump, ν_0 represents the attempted frequency of lithium ion jump to the nearby lattice point, ΔE is the barrier height that lithium ion needs to overcome to migrate to the nearest lattice point. From the above formula (1), it can be seen that lithium ion concentration (cV) plays a very important role in the electrical properties of lithium ion conductors. According to the principle of electroneutrality, additional lithium ions will be introduced into LiTaSiO5 materials when the quadrivalent titanium ion partially replaces the pentavalent tantalum ion in the parent phase LiTaSiO5 material. According to the following Kroger-vink equation:

$$2TiO_2 + 2Ta_{Ta}^{\times} + 2Li_2O \rightarrow 2Ti_{Ta}^{'} + 2Li_i^{g} + Ta_2O_5 \qquad (2)$$

When Ta5+ was replaced by 0.1mol of Ti4+ ions, 0.1mol of lithium ions were introduced into LiTaSiO5 to obtain a new lithium ion conductor Li1.1Ta0.9Ti0.1SiO5 with the structure of sphene. According to the research results of Mohamad M Ahmad in the garnet-like structure Li5La3M2O12 (M=Ta, Nb) lithium ion conductor, not all lithium ions can be migrated, only about 3.9% of lithium ions can migrate in Li5La3M2O12 material and contribute to its electrical properties [13]. It is not difficult to find that there is a higher mobile lithium ion concentration cV in Li1.1Ta0.9Ti0.1SiO5 material.

According to the point defect theory, the concentration of movable defects (lithium ions) is positively proportional to the relaxation peak height [14]. Figure 6 shows the variation curve

of dielectric loss of Li1+xTa1-xTixSiO5 (x=0 and x=0.1) Li-ion conductor material with the test frequency. According to the neutron diffraction fitting results, lithium ions occupy only one lattice point (Li1) in LiTaSiO5 material and are fully occupied, which is consistent with the conclusion that no obvious relaxation peak is found in the dielectric frequency spectrum lines. However, when the accepter of zirconium ion Zr4+ is doped, the distribution state of lithium ions changes, occupying the two lattice positions of Li1 and Li10 respectively and their occupancy rates are 60% and 44%, that is, there are a large number of lithium vacancy ions in the Li1 and Li10 lattice positions [12].

Considering the structural similarity between Li1.1Ta0.9Zr0.1SiO5 and Li1.1Ta0.9Ti0.1SiO5, there are also a large number of lithium vacancies in Li1.1Ta0.9Ti0.1SiO5, which is the reason for the obvious dielectric relaxation peak observed in Li1.1Ta0.9Ti0.1SiO5. Through the comparison of dielectric loss spectra and structural analysis of Li1+xTa1-xTixSiO5 (x=0 and x=0.1) lithium ion conductor materials, it is not difficult to find that there is a higher mobile lithium ion concentration cV in Li1.1Ta0.9Ti0.1SiO5 materials. In addition, according to the analysis discussed above, the activation energy of lithium ion migration and diffusion in Li1.1Ta0.9Ti0.1SiO5 material is 0.31eV ~ 0.35eV, which is lower than the activation energy of lithium ion diffusion and migration in the parent phase LiTaSiO5 material. This indicates that the height of the potential barrier of lithium ion diffusion is reduced to a certain extent through the acceptor doping of titanium ion, which is conducive to the diffusion and migration of lithium ion. Therefore, higher mobile lithium ion concentration and lower migration activation energy are the reasons for the improvement of lithium ion conductivity of Li1.1Ta0.9Ti0.1SiO5 material.

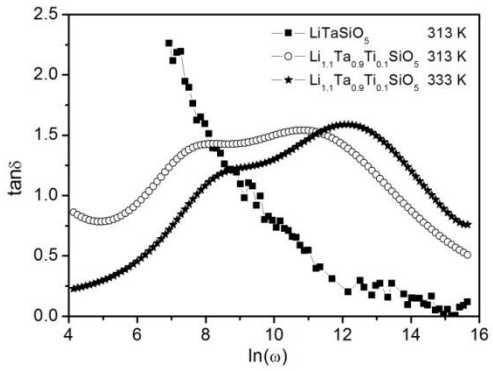

Figure 6: The curves of dielectric loss tanδ versus lnw for the Li1+xTa1-xTixSiO5 (x=0 and x=0.1） sample at the different temperature （313 K and 333 K）

Conclusion

A new lithium ion conductor Li1+xTa1-xTixSiO5(x=0 and x=0.1) was prepared by solid phase reaction method, and the electrical properties of Li1.1Ta0.9Ti0.1SiO5 (x=0.1) were measured by AC impedance tracking. When the temperature is 333 K, the conductivity of Li1.1Ta0.9Ti0.1SiO5 material can reach 1.93 × 10-5 S/cm, which is almost an order of magnitude higher than that of the parent LiTaSiO5 material. Higher concentration of mobile lithium ions and lower activation energy of diffusion and migration are the main reasons for the increase of the conductivity of Li1.1Ta0.9Ti0.1SiO5.

Acknowledgments

This work has been subsidized by the National College Student Innovation and Entrepreneurship Training Project (202210719001), Yan 'an University Research Student Education Innovation Project (YCX2023024).

Reference

[1] Yingqiang Wu, Wenxi Wang, Jun Ming, et al. An exploration of new energy storage system: high energy density, high safety, and fast charging lithium-ion battery, Adv. Funct. Mater. 2019, 29(1): 1805978.

[2] Takeshi Yajima, Yoyo Hinuma, Satoshi Hori, et al. Correlated Li-ion migration in the superionic conductor Li10GeP2S12, J. Mater. Chem. A, 2021,9, 11278-11284.

[3] Hongjie Xu, Guoqin Cao, Yonglong Shen, et al. Enabling argyrodite sulfides as superb solid-state electrolyte with remarkable interfacial stability against electrodes, Energy Environ. Mater. 2022, 5(3):852-864.

[4] Xiaowen Zhan, Shen Lai, Mallory P. Gobet, et al. Defect chemistry and electrical properties of garnet-type Li7La3Zr2O12, Phys. Chem. Chem. Phys. 2018,20: 1447-1459.

[5] Hamid R. Arjmandi, Steffen Grieshammer, Defect Formation and migration in Nasicon Li1+xAlxTi2−x(PO4)3, Phys. Chem. Chem. Phys. 2019,21: 24232-24238.

[6] Xin Guo, Pardha Saradhi Maram, Alexandra Navrotsky, A correlation between formation enthalpy and ionic conductivity in perovskite-structured Li3xLa0.67−xTiO3 solid lithium ion conductors, J. Mater. Chem. A, 2017,5:12951-12957.

[7] Zhu Yizhou, He Xingfeng, Mo Yifei, Origin of Outstanding Stability in the Lithium Solid Electrolyte Materials: Insights from Thermodynamic Analyses Based on First-Principles Calculations, ACS Applied Materials & Interfaces, 2015,7: 23685-23693.

[8] Shan Xiong, Xingfeng He, Aijie Han, et al. Computation guided design of LiTaSiO5, a New lithium ionic conductor with sphene structure, Adv. Energy Mater. 2019, 9:1803821.

[9] Wang Weiguo, Li Xianyu, Liu Ting, and Hao Gangling, Mechanical and dielectric relaxation studies on the fast oxide ion conductor Na0.54Bi0.46TiO2.96, Solid State Ionics, 2016,290:6-11.

[10] Qi Wang, Jian-Fang Wu, Ziheng Lu, Francesco Ciucci, Wei Kong Pang, Xin Guo, A new lithium-ion conductor LiTaSiO5: theoretical prediction, materials synthesis, and ionic conductivity, Adv. Funct. Mater. 2019, 29(37): 1904232.

[11] Wang Xianping, Fang Qianfeng, Mechanical and dielectric relaxation studies on the mechanism of oxygen ion diffusion in La2Mo2O9, Phys. Rev. B, 2002,65,064304 (6 pages)

[12] Zhao Qinfu, Guo Jianpeng, Su Mengyu, et al. Design Principles for Rotational Cluster Anion [BH4]− Promote Superionic Conductivity in Sodium-Rich Antiperovskite Na3OBH4, J. Phys. Chem. C, 2022, 126(38): 16546–16555.

[13] Mohamad M Ahmada, Enhanced lithium ionic conductivity and study of the relaxation and giant dielectric properties of spark plasma sintered Li5La3Nb2O12 nanomaterials, Ceramics International, 2015, 41:6398-6408.

[14] A. S. Nowick and B. S. Berry, Anelastic Relaxation in Crystalline Solids (Academic, New York, 1972).